Effect of $CoCl_2$ Doping on the Optical and Electrical Properties of PEO Polymer Films for Optoelectronic Applications

Roopa K. V., Subramanya Kilarkaje *

Department of PG Studies and Research in Physics, Kuvempu University, Shivamogga, Karnataka, India

Editor's note: Polyethylene oxide (PEO) films are characterized by their semi-crystalline structure, which imparts several important properties, including hydrophilicity, chemical stability, solubility in alcohols, and flexibility. However, the absence of charge carriers limits their application in various fields. Enhancing the conductivity of these films could lead to advancements in next-generation photonic devices, solar cells, optoelectronics, and sensors. Roopa K. V. and Subramanya K. investigated the doping of PEO films with cobaltous chloride ($CoCl_2$) at various concentrations. Their findings indicated that the interaction between Co^{2+} ions and the ether groups of PEO results in the formation of metal-ligand coordination bonds within the doped PEO films. This interaction significantly enhances the electrical conductivity and ion mobility of the $CoCl_2$-doped PEO films and results in a redshift in the absorption edge of these films.

doi: 10.22034/jams.2025.210147

How to cite: R. K.V. and S. Kilarkaje, *Journal of Applied Material Science*, **2025**, *1*, 210147.

JOURNAL OF
APPLIED
MATERIAL
SCIENCE
jams.hsu.ac.ir

Journal of Applied Material Science **2025**, *1*, 210147
How to cite: R. K.V. and S. Kilarkaje, *Journal of Applied Material Science*, **2025**, *1*, 210147.
Journal homepage: **jams.hsu.ac.ir**

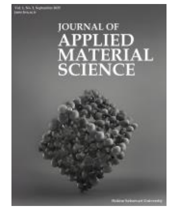

Original Research

Effect of $CoCl_2$ Doping on the Optical and Electrical Properties of PEO Polymer Films for Optoelectronic Applications

Roopa K. V., Subramanya Kilarkaje *

Department of PG Studies and Research in Physics, Kuvempu University, Shivamogga, Karnataka, India

Abstract

Highly porous polymer films were synthesized using the solution casting technique by doping polyethylene oxide (PEO), a semi-crystalline polymer known for its good film-forming ability, chemical stability, ionic conductivity, and optical properties, with varying concentrations of cobaltous chloride ($CoCl_2$) (0, 5, 10, 15, and 20 wt%). $CoCl_2$, a transition metal halide containing Co^{2+} ions, is known for its tunable optical absorption, enhanced electrical conductivity, and strong coordination behavior, making it suitable for improving the performance of polymer matrices. X-ray Diffraction analysis revealed a gradual reduction in crystallinity with increased $CoCl_2$ content, indicating structural disruption and confirming (120) and (032) planes as per JCPDS standards. Fourier transform infrared (FTIR) spectra showed interactions between Co^{2+} ions and PEO ether groups, suggesting the formation of metal-ligand coordination bonds. UV-Visible spectroscopy exhibited a redshift in the absorption edge, and Tauc's plots revealed decreasing direct and indirect band gaps. The extinction coefficient increased significantly (from 1×10^4 to 6.7×10^4), indicating enhanced light absorption and suitability for UV photodetector applications. AC conductivity increased with doping due to enhanced ion mobility, while Nyquist plots confirmed reduced bulk resistance and improved ion transport through hopping mechanisms. The 20 wt% $CoCl_2$-doped film exhibited a bulk resistance of just 33 Ω, indicating potential semiconductor or ionic conductor behavior. SEM images confirmed increased surface porosity and morphological changes, consistent with the semi-crystalline nature of the films. These findings suggest that $CoCl_2$-doped PEO films are promising candidates for flexible electronics, optoelectronic devices, sensors, and solid polymer electrolytes in energy storage applications.

Keywords: Polyethylene oxide; Inorganic metal salt; Polymer composite film; Energy band gap; FTIR; AC Conductivity.

1. Introduction

Polymers have established themselves as unbelievable and non-replaceable across diverse fields due to their physical flexibility, low price, weightlessness, processing ease, and chemical tunability. They are widely used in household products, adhesives, medical, and pharmaceutical industries. Properties such as non-toxicity, porosity behavior, flexibility, and solubility in desired solvents make them particularly suitable for functional applications. Furthermore, their

* Corresponding author.
Email addresses: subbuk17@gmail.com, drskkuphysics@gmail.com (S. Kilarkaje)

Received 30 July 2025
Revised 8 August 2025
Accepted 9 August 2025
Available online 10 August 2025

https://doi.org/10.22034/jams.2025.210147

covalent backbone allows polymers to interact with dopants and fillers effectively, enabling structural and functional modifications for specific performance requirements [1].

Among many polymers, polyethylene oxide (PEO) is suitable for flexible photonic applications for its chemical structure, covalent bond at the backbone, its semi-crystalline nature, hydrophilicity, chemical stability, solubility in alcoholic groups, and flexibility [2]. Although PEO is electrically not capable of conducting alone, it lacks charge carriers for performing strong optical, electrical responses in advanced applications such as solar cells, optoelectronics [3]. Further development of polymer and combined constituent materials, various strategies have been found. Among these, doping, adding a small portion of metal salts to the main polymer structure, enhances optical, electrical properties. This occurs due to a modification in microlevel structure, which is not much explored in the present era. The ability to solubilize a range of inorganic salts makes it highly adaptable for material blending and conductivity enhancement [4].

To overcome the intrinsic limitations of PEO for electronic applications doped with transition metal salts. Cobaltous chloride ($CoCl_2$), a pink crystalline salt, a transition metal halide containing Co^{2+} ions, due to partially filled d-orbitals, exhibits optical absorption. Modification in structure forming tetrahedral or octahedral complexes is one such candidate known for its conductive properties, transition metal activity, and coordination behavior. $CoCl_2$ dissolves in alcohol also chemically stable, exhibiting partially filled d orbit with stability, and is easy to incorporate into polymer structures [5]. When integrated with PEO, $CoCl_2$ can act as a donor species, modifying the charge distribution, enhancing free carrier density, and improving both structural and electrical performance of the polymer system [3].

Dopant significantly influences the overall work frame of the application chosen and helps in tuning of microstructure property, leading to UV-Vis absorbance, XRD, FTIR, electrical property, and scanning electron microscopy (SEM), leading to the formation of polycrystalline domains that are advantageous for charge transport and mechanical strength. There is no such work framework accessing inter-connected research work accessing with dopant $CoCl_2$ induced with PEO. There exists a narrow gap correlating with multifunctional characteristic studies, enhancing properties [6].

To address the above research gap present study reports on the fabrication and characterization of PEO-$CoCl_2$ films via the solution cast technique, a low-cost, durable method. This is subjected to multi-characterization techniques such as UV-Visible spectroscopy, XRD, FTIR, SEM, and AC electrical conductivity, enhancing photonic applications. In the context of these resulting optical responses, bonding behavior, contact angle-volume measurement, bonding behavior, crystal size, nature of structure, morphology, and charge transport of the film are considered. Their processability at room temperature, compatibility with flexible substrates, and potential for miniaturization make them ideal for next-generation applications such as flexible displays, low-power sensors, optoelectronics, and renewable energy devices [7].

This work reveals Co^{2+} ions of dopant responsible for charge transport, aiming to differ in the result of absorption-extinction coefficient and refractive index by reducing the optical band gap below 3eV. FTIR reveals Co=O bond and C=O coordination bond, XRD reveals (120) and (032) planes, and crystal size. The SEM analysis has been revised to better correlate with the above findings, providing morphological evidence that supports the structural and electrical characteristics discussed. AC conductivity enhances, and the resistance of the material decreases to 0.33Ω. This evidence suggests PEO-$CoCl_2$ films potential candidate for use in photonics applications. The structural, optical, and electrical properties of the composite films are systematically investigated using UV–Visible spectroscopy, FTIR, XRD, SEM, and AC electrical I–V characterization. This study focuses on how varying $CoCl_2$ concentrations affect optical band gap, crystallinity, and conductivity with a view toward applications in photoactive systems, sensors, and energy storage devices [8].

2. Experimental

2.1. Materials

The Solution cast technique method is preferred to achieve Polyethylene Oxide (PEO, Mw = 5.6×10^6 g/mol, Merck) and Cobaltous Chloride ($CoCl_2$, Mw = 237.93 g/mol) doped films, were to its simplicity, cost-effectiveness, and ability to yield uniform films under constant temperature 50 °C. A fixed amount of PEO was dissolved in methanol (Mw = 32.04 g/mol; SD Fine Ltd.) under constant stirring to obtain a clear solution at 50 °C. $CoCl_2$ was added in varying concentrations (0%, 5%, 10%, 15%, and 20% by weight of PEO) and stirred thoroughly to ensure homogeneity and uniformity under thermal conditions of 50 °C. The resulting solution was cast into Petri dishes and dried at a temperature of 50 °C to allow solvent evaporation and avoid thermal degradation of the sample. Thus, the obtained samples are sealed in zip cover bags and desiccated. The films were cut into squares of one square centimetre, and characterization was carried out.

2.2. Measurements

The optical properties were studied using UV–visible NIR spectroscopy using a Quartz tungsten Halogen lamp as a source for pure and composites between 200 nm to 1500 nm wavelength range to determine band gap values. Fourier-transform infrared (FT-IR) spectroscopy was conducted in KBr medium using a Perkin Elmer IR Spectroscopy in the air medium. The structural properties of the synthesized samples were analyzed using an X-ray diffractometer with Cu-Kα radiation (λ = 1.5406 Å), operating at 40 kV and 30 mA, with a scan range from 5° to 80° (2θ), and a step size of 5° per minute. Surface morphology studies and thickness of the sample were studied using Table top Scanning electron microscope (SEM), with a JEOL JSM-IT500LA microscope operating at 5000V, and at a resolution of 300X magnification was taken under vacuum. AC Electrical property studies were done using a Keithley Source Measure, frequency versus dielectric.

3. Results and discussion

3.1. UV-Visible spectroscopy results

UV-Vis spectroscopy, which studies the interaction of electromagnetic radiation with matter, is a primary method for analyzing absorbance, transmittance, band gap, and optical properties of materials. Figure 1 shows strong absorbance peaks between 570–750 nm, corresponding to the visible red/near-infrared region, indicating that these wavelengths are absorbed while blue/violet light is reflected, resulting in a bluish-violet film appearance. There is a possibility of forming both tetrahedral (blue/violet) and octahedral (violet/pink) of Co^{2+}ionscoordination complexes with the polyethylene oxide (PEO) matrix [9-11].

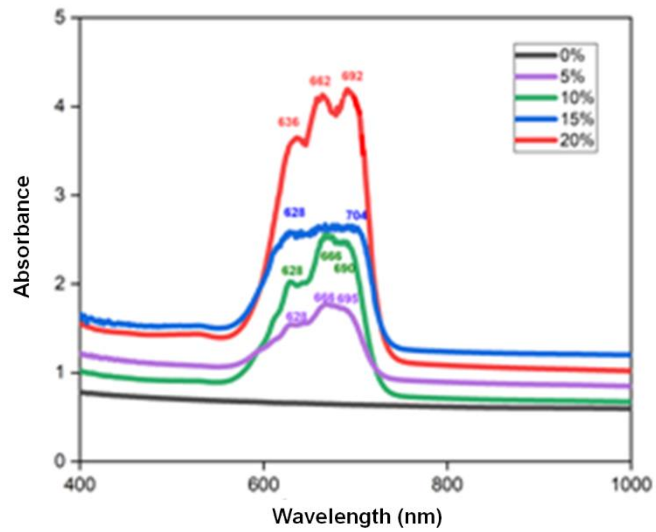

Figure 1. UV-Vis absorption spectra of the samples with varying dopant concentrations (0%, 5%, 10%, 15%, and 20%) in the range of 400–1000 nm.

Table 1 exhibits the data for pure PEO, the $CoCl_2$-doped sample, as observed increased absorbance, absorption coefficient, and extinction coefficient, along with enhanced translucency, indicating higher crystallinity and formation of tetrahedral Co^{2+} complexes [12]. Figure 2 shows correlated Tauc plots and their derivative using equations (1) and (2), showing a reduction in direct band gap (<3 eV) with increased $CoCl_2$ concentration. At longer wavelength absorption, UV sensitivity is seen sensitive at longer wavelength absorption, which makes the material suitable for photosensitive applications [13, 14].

Table 1. Direct and Indirect Band Gap, Absorption Coefficient, Extinction Coefficient, and Refractive Index of doped PEO–$CoCl_2$ films

Dopant Weight Percent (%)	0	5	10	15	20
Direct Band Gap (eV)	3.20	1.93	1.78	1.61	1.55
Indirect Band Gap (eV)	2.40	1.90	1.65	1.51	1.05
Absorption Coefficient (eV)	-	1.688	1.683	1.647	1.632
Extinction Coefficient ($\times 10^{-4}$)	0.95	1.47	1.65	3.21	3.66
Refractive index	0.11	0.18	0.22	0.28	0.66

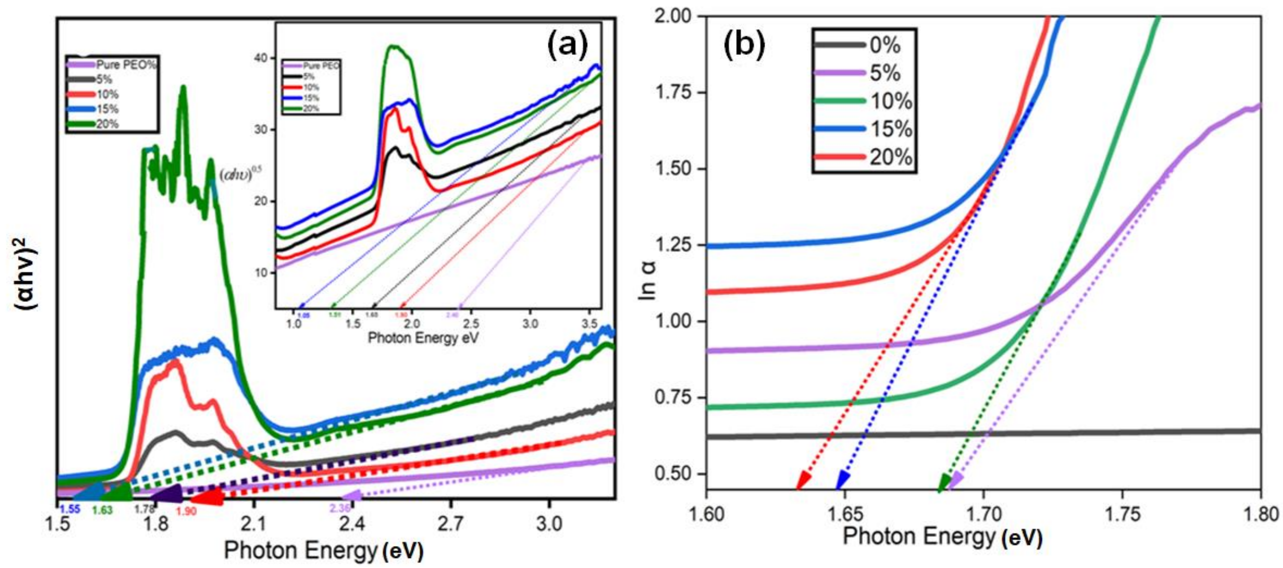

Figure 2. Plots of the direct and indirect band gaps (a), as well as the absorption coefficient (b), as a function of increasing dopant weight percentage.

Beer–Lambert Law address calculation for absorption coefficient (α) via equation (3), showing enhancement, reflecting the material's photon absorption strength as in Figure 2. Figure 3 shows that the extinction coefficient increased from 0.95×10^{-4} to 3.66×10^{-4} with increased doping, calculated using equation (4), indicating photon penetration at higher photon absorption. The refractive index, calculated via equation (5), increased from 0.11 to 0.66 as in Figure 3, implying improved polarizability and photon trapping at grain boundaries, supporting increased optical conductivity [15-17]. A summary of the optical data is presented in Table 1.

$$\alpha h\nu = A(h\nu - E_g)^n \quad (1)$$

$$\alpha = 2.303(t^{-1})log(T)^{-1} \quad (2)$$

$$\alpha = \frac{2.303A}{t} \quad (3)$$

$$k = \frac{\alpha\lambda}{4\pi} \quad (4)$$

$$n = \sqrt{\frac{(1+R)^2 - k^2}{(1-R)^2 + k^2}} \quad (5)$$

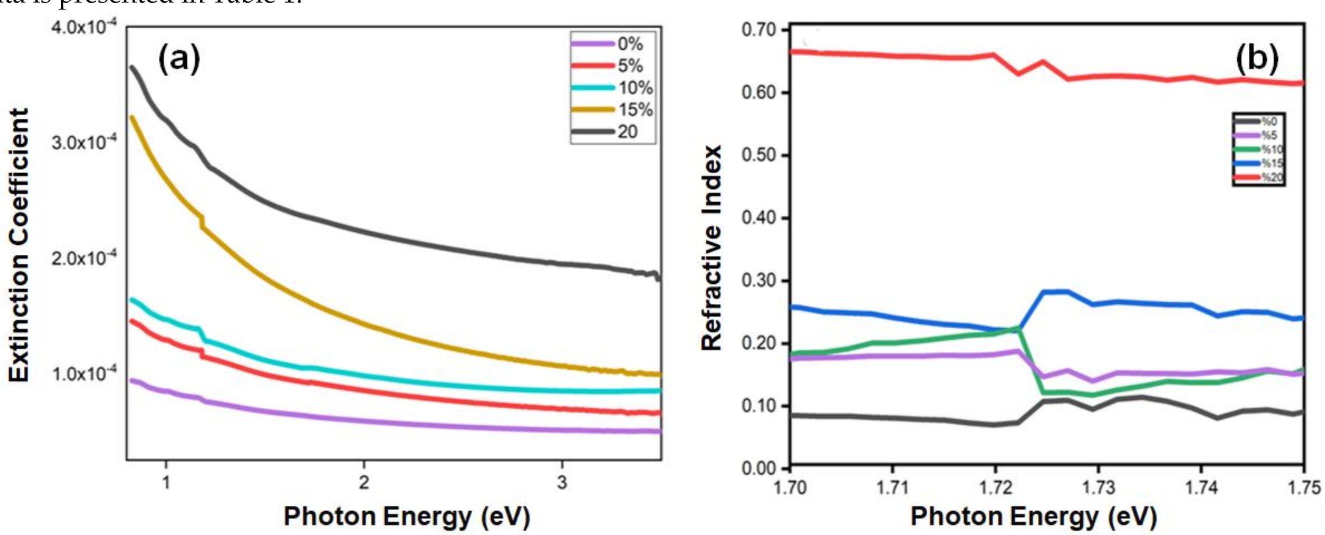

Figure 3. Plots of the extinction coefficient and refractive index as functions of increasing dopant weight percentage.

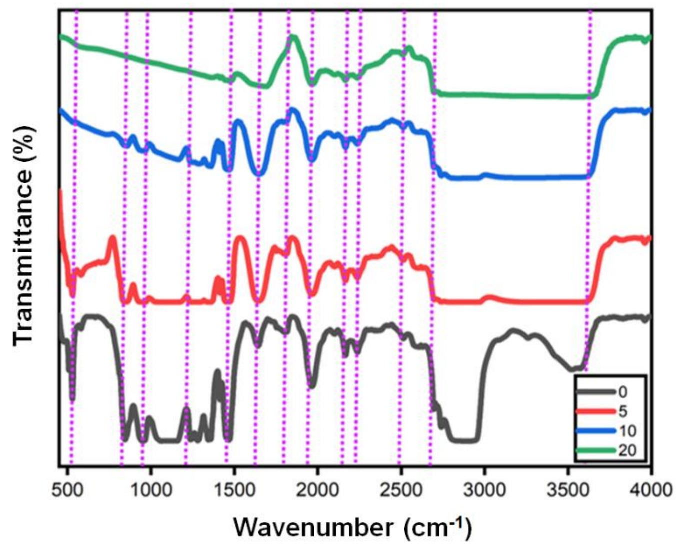

Figure 4. FTIR spectra of samples with varying $CoCl_2$ dopant concentrations (0%, 5%, 10%, and 20%) in the wavenumber range of 500–4000 cm^{-1}.

3.2. Fourier transform infrared spectroscopy studies

FTIR data predicts formation of new bonds in the doped PEO–$CoCl_2$ films at higher concentration, which are absent in pure PEO, evidencing structural modifications upon doping. In Figure 4, the broad O–H stretching band is seen in all the samples around 3500 cm^{-1}, confirming hydroxyl interactions [6, 18]. Similar to OH stretching, symmetric CH_2 stretching vibration characteristic near 2900 cm^{-1} in pure PEO disappears in doped samples, which hinders the structural organization due to coordination between Co^{2+} ions and the PEO matrix [19].

CH bending and stretching vibrations near 2600 cm^{-1} are observed in all samples, indicating a Carbon-Hydrogen bond. C≡C stretching exists around 2100–2260 cm^{-1}, while peaks from 1800–1900 cm^{-1} and near 2250 cm^{-1} are attributed to CO–Co metal carbonyl bonds, confirming the formation of Co^{2+} complexes [20].

An absorption peak around 1900 cm^{-1} is assigned to C=O stretching, and a band near 1600 cm^{-1} indicates symmetric and asymmetric C=C and O=C=O stretches, suggesting the presence of metal carboxylate complexes. Additionally, peaks around 1300 cm^{-1} are related to C–O stretching of alcohol groups and CH_2 wagging. The CH_2–CH_2–O group, prominent in pure PEO, diminishes

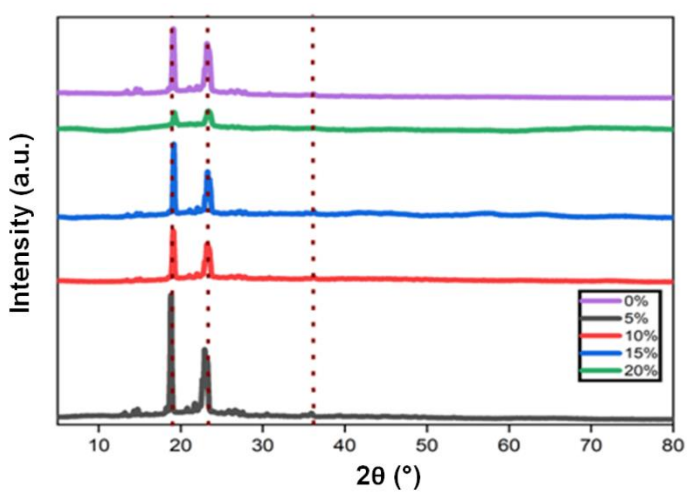

Figure 5. XRD patterns of samples with varying $CoCl_2$ dopant concentrations (0%, 5%, 10%, 15%, and 20%).

at higher dopant concentrations, suggesting that tetrahedral Co^{2+} complexes interact with the polymer's carbon groups, altering the polymer's local structure [21, 22]. FTIR reveals metal ligand coordination bond with peaks around 2250 cm⁻¹ (CO–Co metal carbonyls) and 2100–2260 cm⁻¹ (C=C stretching), which were absent in pure PEO.

3.3. X-ray diffraction analyses

Figure 5 shows that the undoped PEO exhibits two sharp peaks at 2θ ≈ 19.2° and 23.3°, corresponding to the (120) and (032) planes, respectively, as per JCPDS standards. These intense reflections confirm the semi-crystalline nature of pure PEO.

The sharp, high-intensity peaks at 2θ ≈ 19.2° and 23.3° in Figure 5 confirm the semi-crystalline nature of pure PEO, indicating well-ordered chain packing. With increasing $CoCl_2$ dopant concentration, these peaks persist but exhibit broadening and reduced intensity, suggesting decreased crystallinity due to structural distortion [23, 24].

This reduction is attributed to Co^{2+} ions interacting with ether oxygen in PEO via coordination bonds, disrupting chain alignment and inducing a shift toward amorphous character.

The reduced crystallinity enhances ion mobility and flexibility, improving charge transport-crucial for applications in flexible electronics, solid-state batteries, and optoelectronic devices.

Table 2, tabulation of structural parameters of XRD, such as degree of crystallinity (Xc), average crystallite size (P), and inter-crystallite separation (R), was calculated using:

$$P = 0.9\lambda / (\beta \cos\theta) \tag{6}$$

$$R = 5\lambda / (8 \sin\theta) \tag{7}$$

where $\lambda = 1.5 \times 10^{-10}$ m and β is the full width at half maximum (FWHM).

This structural evolution aligns with UV-Vis, SEM, and FTIR findings, which show enhanced light absorption, porous morphology, and altered bonding. The reduced crystallinity enhances ion mobility and flexibility, improving charge transport-crucial for applications in flexible electronics, solid-state batteries, and optoelectronic devices.

3.4. SEM morphology studies

Figure 6 presents the scanning electron micrographs of pure PEO and PEO–$CoCl_2$ composites (with 5% and 15% $CoCl_2$) recorded at 5000 V, ×3500 magnification, 5 µm scale, and SEI mode (18 46). Figure 6, Pure PEO has an amorphous appearance, smooth, and looks homogeneous surface. Increased dopant concentration shows a non-homogeneous, spike-like structure, rough surface with an increase in the number of porosities throughout the film also agglomerated Cobalt salt matrix. The linear structure of PEO is evidenced, and the concentration of dopant shows an increased PEO-$CoCl_2$matrix form. The porosity is due to the effect of temperature, which elevates coordination complex formation. Increased Co^{2+} ion and matrix help in evidencing increased conductivity. This is evidenced by the optical property showing particle penetration within

Table 2. Summary of XRD parameters for samples with varying increased $CoCl_2$ dopant weight percentages

Dopant Weight Percent (%)	2θ (°)	θ (°)	d-spacing	P (Å)	R (Å)
0	19.10	9.55	4.645	6.65	7.50
	23.26	11.63	3.841	9.89	1.16
	36.26	18.13	2.466	3.50	1.42
5	18.86	9.43	4.711	8.79	1.79
	22.83	11.41	3.878	3.24	1.02
	36	18	2.492	1.99	1.24
10	18.97	9.48	4.643	6.61	1.55
	23.26	11.63	3.833	1.78	1.16
	36.13	18.06	2.481	6.21	1.32
15	19.23	9.61	4.630	8.95	4.95
	23.26	11.63	3.786	2.22	1.16
	36.26	18.13	2.4776	7.01	1.42
20	19.36	9.68	4.616	6.81	3.71
	23.39	11.69	3.770	2.04	1.22
	36.39	18.19	2.4770	4.75	1.53

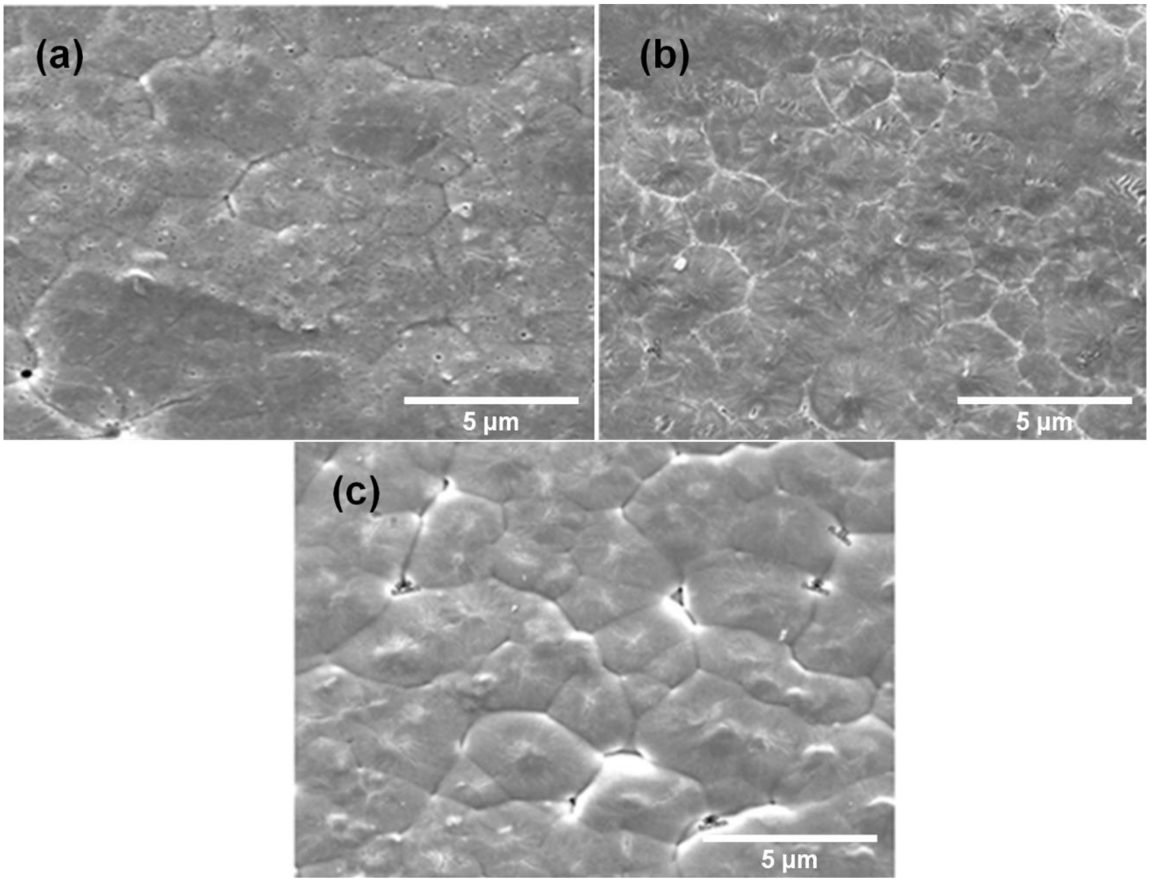

Figure 6. SEM images of Pure PEO (a) and PEO films doped with 5% (b) and 15% (c) $CoCl_2$ concentrations.

the sample is enhanced, allowing charges to pass, hence the conductivity of the sample is possible [25, 26].

3.5. Electrical characterisations

AC conductivity studies confirm enhanced charge transport within the doped PEO–$CoCl_2$ films, as conductivity is inversely proportional to resistivity-reflecting reduced opposition to charge flow. Figures 7 and 8 (Cole–Cole plot) are plotted for Z' versus Z" as a function of frequency, illustrating the trend of a semicircle that implies the Debye model, showing an increase in bulk resistance at Pure PEO 0.3×10^6 Ω. At a higher weight percentage, it does not follow a semicircle path, hence does not obey the Debye-Model type; also, Bulk resistance decreased to 0.33 Ω, implying that there exists a hopping conduction mechanism. This improvement is attributed to the increased mobility of ionic species introduced by Co^{2+} doping, which facilitates charge transport along the polymer chains.

According to Equation (8), electrical conductivity (σ) is calculated. AC electrical conductivity increases with dopant concentration [6, 27], as tabulated in Table 3. This observation aligns with UV-Vis results, where a reduced band gap and denser film colour-due to higher Co^{2+} content, indicate improved ion transport and enhanced charge flow throughout the film. This is attributed to low-power optoelectronics and sensor devices.

$$\sigma = \frac{d}{RA}^{n} \tag{8}$$

Table 3. Electrical resistance of samples at varying dopant concentrations (0–20 wt%)

Dopant Weight Percent (%)	0	5	10	15	20
Resistance (Ω)	3.88×10^6	1.527×10^3	2.36×10^2	48.01	0.33
Electrical Conductivity (S/cm)	1.55×10^{-8}	3.93×10^{-5}	2.54×10^{-4}	1.25×10^{-3}	1.18×10^{-1}

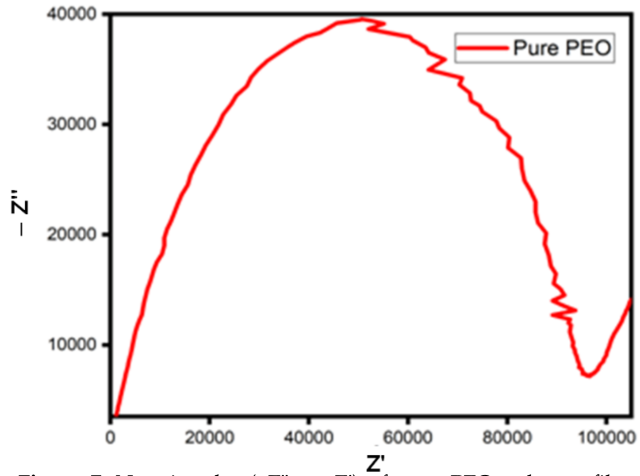

Figure 7. Nyquist plot (–Z″ vs. Z′) of pure PEO polymer film, showing a characteristic semicircular arc, indicating the bulk resistance and conductivity behavior.

4. Conclusions

$CoCl_2$-doped PEO polymer films exhibit enhanced optical and electrical properties, making them strong candidates for use in electronic, optical-sensitive, and optoelectronic applications. The doping process leads to increased absorbance, absorption coefficient, and extinction coefficient from 0.95×10^{-4} to 3.66×10^{-4}, indicating optical sensitivity and significant modifications in direct band gap from 3.20eV to 1.55eV and indirect band gap energies, refractive index found to be 0.66 with 20% dopant concentration, and optical conductivity.

With rising $CoCl_2$ concentrations, improved bonding interactions, greater hydrophilicity, and enhanced dispersion of Co^{2+} ions are observed, as supported by contact angle and colorimetric analyses. FTIR studies confirm the formation of new bonding environments and the incorporation of Co^{2+} ions within the polymer matrix, contributing to improved charge carrier density. Disappearance of peaks of CH_2 symmetric stretches evidencing new bonding interactions induced in the polymer structure. These structural changes are directly correlated with the electronic properties of the sample.

XRD analysis reveals 19° and 23° are seen at all concentration ranges, depicting well-ordered chain packing, reduced crystallinity, variations in crystal size, and changes in interplanar spacing with increased doping, indicating structural transformation within the polymer network. Porosity, grain size, and agglomerated

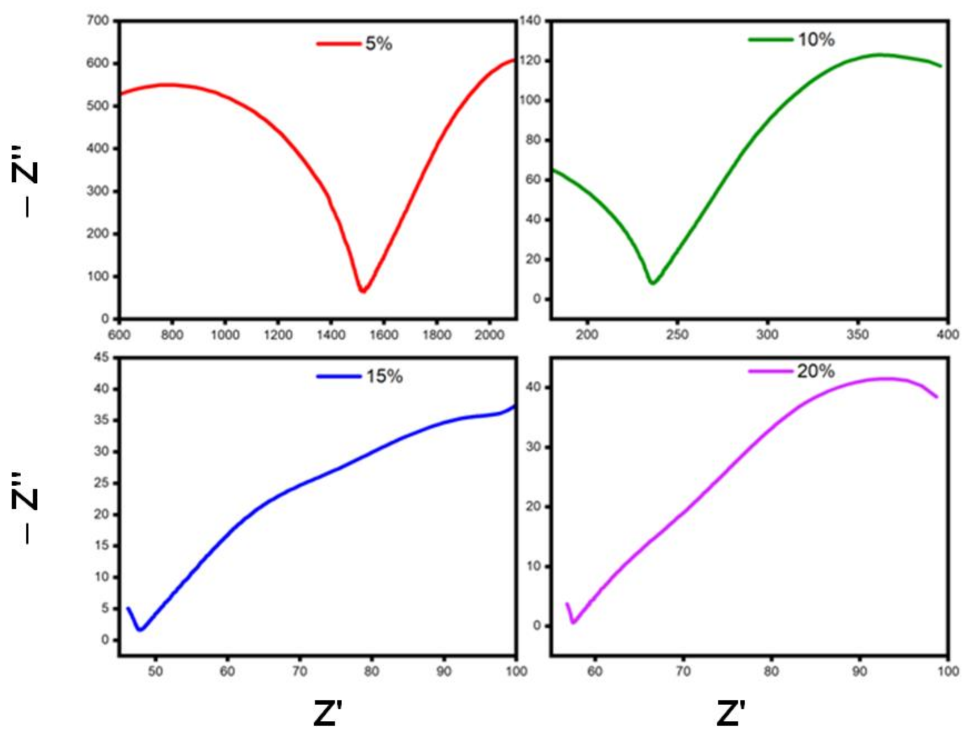

Figure 8. Nyquist plots (–Z″ vs. Z′) of $CoCl_2$-doped PEO films at different doping concentrations (5%, 10%, 15%, and 20%).

ions of the polymer matrix are enhanced, as verified by SEM analysis. Electrical measurements demonstrate a notable decrease in resistivity and Debye-Model type, which corresponds increase in AC conductivity, suggesting enhanced ionic mobility, disorder in the structural bond, and charge transport.

Overall, the modified PEO–$CoCl_2$ films show promising potential for UV-sensitive, flexible, and cost-effective applications in solar cells, photodetectors, and other optoelectronic devices.

Acknowledgments

The authors acknowledge Sahyadri Science College, Kuvempu University, for fabrication facilities. Appreciation is extended to Dr. Praveen K. C. (LEOS–ISRO) for UV-NIR spectroscopy, Prof. Ganesh Sanjeev (Mangalore University) for AC conductivity studies, and Prof. Balram Sahoo (IISc Bangalore) for XRD analysis.

Conflict of Interest

The authors declare no conflict of interest.

References

1. K.V. Roopa, et al. Study the effect of cobalt chloride (CoCl2) on the structural, optical, and electrical properties of polymer electrolyte (PVA-CoCl2) films. *IOP Conference Series: Materials Science and Engineering*, **2024**, *1300*, 012017.

2. S.S. Siwal, et al. Recent advancements in transparent carbon nanotube films: chemistry and imminent challenges. *Journal of Nanostructure in Chemistry*, **2021**, *11*, 93.

3. A.D. Telfah, et al. Optical, electrical, and structural properties of polyethylene oxide/fullerene nanocomposite films. *Physica B: Condensed Matter*, **2024**, *679*, 415787.

4. S. Kamal, et al. Synthesis of boron doped C3N4/NiFe2O4 nanocomposite: An enhanced visible light photocatalyst for the degradation of methylene blue. *Results in Physics*, **2019**, *12*, 1238.

5. S.B. Aziz, et al. Structural, thermal, morphological and optical properties of PEO filled with biosynthesized Ag nanoparticles: New insights to band gap study. *Results in Physics*, **2019**, *13*, 102220.

6. M.G. Tadesse, A.S. Ahmmed, and J.F. Lübben. Review on Conductive Polymer Composites for Supercapacitor Applications. *Journal of Composites Science*, **2024**, *8*, 53.

7. Z. Gu, et al. From planar structures to curved optoelectronic devices: The advances of halide perovskite arrays. *Matter*, **2023**, *6*, 2666.

8. M. Ahmadi, et al. From Unregulated Networks to Designed Microstructures: Introducing Heterogeneity at Different Length Scales in Photopolymers for Additive Manufacturing. *Chemical Reviews*, **2024**, *124*, 3978.

9. D. Patel, et al. A Review on UV Visible Spectroscopy. *International Journal of Creative Research Thoughts*, **2022**, *10*, 2320.

10. S. Agrahari, S.P. Singh, and A.K. Gupta. DFT analysis of structural and optoelectronic properties of (PEO)8-LiFSI complexes. *Ionics*, **2024**, *31*, 3053.

11. A. Patil and N. Patil. Synthesis, Characterization and Conductance Properties of Cobalt Chloride Doped Polyvinyl Alcohol / Polythiophene (PVA-Co-Pth) Nanocomposite Films. *Journal of Materials Science and Surface Engineering*, **2022**, *9*, 1051.

12. I.N. Perera, et al. Enhanced Electrochemical Properties of Cobalt by Varying the Ethylene Glycol - Choline Chloride Composition in a Deep Eutectic Solvent Mixture. *Journal of The Electrochemical Society*, **2023**, *170*, 052503.

13. J.G. Doremus, et al. Photocatalytic applications of covalent organic frameworks: synthesis, characterization, and utility. *Nanoscale*, **2024**, *16*, 21619.

14. S. Guzman-Puyol, J.J. Benítez, and J.A. Heredia-Guerrero. Transparency of polymeric food packaging materials. *Food Research International*, **2022**, *161*, 111792.

15. K. Charradi, et al. Fabrication and Characterization of Polyvalent Metals/Oxidized Polyvinyl Alcohol Hybrid Films with Improved Proton Conductivity and Optical Performances. *Journal of Polymers and the Environment*, **2023**, *31*, 3167.

16. M. Tüfekçi, et al. Long-term antifouling surfaces for urinary catheters. *Journal of Materials Chemistry B*, **2024**, *12*, 5711.

17. R. Tanwar, et al. Development and characterization of PVA-starch incorporated with coconut shell extract and sepiolite clay as an antioxidant film for active food packaging applications. *International Journal of Biological Macromolecules*, **2021**, *185*, 451.

18. M.S. Anula and C. BeskeyJob. Growth, Spectral, Optical, Thermal, Mechanical and Dielectric properties of CdCl2 added (Na)2 SbF5 Single Crystals. *Journal of Pharmaceutical Negative Results*, **2023**, *14*, 2432.

19. K.-Y. Hsiao, et al. Identification of Hydroxyl and Polysiloxane Compounds via Infrared Absorption Spectroscopy with Targeted Noise Analysis. *Polymers*, **2025**, *17*, 1533.

20. A.S. De León and S.I. Molina. Influence of the Degree of Cure in the Bulk Properties of Graphite Nanoplatelets Nanocomposites Printed via Stereolithography. *Polymers*, **2020**, *12*, 1103.

21. J.H. Koo, et al. Recent advances in soft electronic materials for intrinsically stretchable optoelectronic systems. *Opto-Electronic Advances*, **2022**, *5*, 210131.

22. A.M. Hawkar, A.M. Pshko, and B.A. Shujahadeen. Investigation of optical band gap in PEO-based polymer composites doped with green-synthesized metal complexes using various models. *RSC Advances*, **2025**, *15*, 23319.

23. M. Khan, et al. Conductive Polymer-Based Electronics in Additive Manufacturing: Materials, Processing, and Applications. *Advances in Polymer Technology*, **2025**, *2025*.

24. S.S. Khasraw, et al. PEO Based Nanocomposite With Improved Structural and Optical Properties. *Journal of Inorganic and Organometallic Polymers and Materials*, **2025**.

25. A. Shahab Marf, R. M. Abdullah, and S. B. Aziz. Structural, Morphological, Electrical and Electrochemical Properties of PVA: CS-Based Proton-Conducting Polymer Blend Electrolytes. *Membranes*, **2020**, *10*, 71.

26. B.A. Abdulkadir, et al. Optimization of the Electrochemical Performance of a Composite Polymer Electrolyte Based on PVA-K2CO3-SiO2 Composite. *Polymers*, **2020**, *13*, 92.

27. A. Kumar, et al. Ion transport, dielectric, and electrochemical properties of sodium ion-conducting polymer nanocomposite: application in EDLC. *Journal of Materials Science: Materials in Electronics*, **2020**, *31*, 10873.